Newania carbonatites, Western India: Example of mantle derived magnesium carbonatites

ARTICLE *in* MINERALOGY AND PETROLOGY · MARCH 2009

Impact Factor: 1.35 · DOI: 10.1007/s00710-009-0076-z

3 AUTHORS:

Anna Doroshkevich
Sobolev Institute of Geology and Mineralogy
30 PUBLICATIONS **124** CITATIONS
SEE PROFILE

G. S. Ripp
Russian Academy of Sciences
44 PUBLICATIONS **157** CITATIONS
SEE PROFILE

Shrinivas G. Viladkar
Carbonatite Research Centre, Amba Dongar
44 PUBLICATIONS **481** CITATIONS
SEE PROFILE

Miner Petrol (2010) 98:283–295
DOI 10.1007/s00710-009-0076-z

ORIGINAL PAPER

Newania carbonatites, Western India: example of mantle derived magnesium carbonatites

Anna Gennad'evna Doroshkevich · German Ripp · Shrinivas Viladkar

Received: 18 November 2008 / Accepted: 28 July 2009 / Published online: 8 August 2009

Abstract The key mineralogical features of the Newania carbonatites, that illustrate their derivation from primary mantle melts (Gruau et al. Terra Nova, Abstract Suppl 1:336, 1995; Viladkar Petrology 6(3):272–283, 1998; Basu and Murty Abstracts of Goldschmidt Conference A40, 2006), are the presence of magnesite, graphite and Cr-rich magnetite. Magnesite is an early crystallizing phase. Cr-rich magnetite and graphite coexist with carbonatite minerals and precipitated from carbonate magma. Graphite, as well as gaseous CO_2 and carbonate minerals such as dolomite and magnesite, can be stable in peridotite mantle. Coexistence of these minerals is controlled by fO_2 and PT-conditions. Mineral geothermometers for the Newania carbonatite give temperatures from 463 to 950°C. The parental source for Newania carbonatites was characterized by a relatively high log (fHF/fH$_2$O) level which increased during the crystallization history of Newania. The estimated oxygen fugacity (for ilmenite–magnetite pairs) varies from −1.5 to +3.5 (log-bar unit deviation from FMQ buffer), which is supported by the presence of Fe-columbite, and the composition of phlogopite, amphibole and pyroxene that have an elevated concentration of Fe^{3+}. However, the oxygen fugacity range represented by co-existing early-crystallized graphite and magnesite is below that of the FMQ buffer and lies on the CCO buffer.

Editorial handling: K. R. Moore

A. G. Doroshkevich (✉) · G. Ripp · S. Viladkar
Geological Institute SB RAS,
Ulan-Ude, Russia
e-mail: ripp@gin.bscnet.ru

Introduction

The Newania carbonatite complex is situated 40 km east of Udaipur, within the 2.5 Ga old Aravalli Rift of Rajasthan (Verma and Greiling 1995), which strikes NE–SW for a distance of >600 km. Mishra (1982) defined two prominent NE–SW lineaments within the Aravalli Rift, which host the major hydrothermal base metal deposits. Mineralization is also associated with the Newania carbonatite in the form of disseminated, uraniferous pyrochlore (20% to 22% U_3O_8, Viladkar et al. 1993), hydrothermal copper (chalcopyrite and malachite) and traces of Gold.

The carbonatitic nature of the Newania complex was first recognized by Dar (1964) during prospecting for the Atomic Energy Minerals Division, and was later confirmed by Deans (unpublished report). An initial investigation of the economic potential of the carbonatites at Newania indicated reserves of about 1 million tones of apatite (6–10 wt% P_2O_5), which was subsequently mined by the State Geological Survey for several years. Phadke and Jhingran (1968) described the geology and petrography of the carbonatite outcrops, and Viladkar and Wimmenauer (1986) and Viladkar and Pawaskar (1989) obtained detailed mineralogical, petrological and geochemical data for the carbonatites, and fenites, respectively.

Deans and Powell (1968) reported a Proterozoic K–Ar date of 959±24 Ma for amphibole from the carbonatite. More recently, Gruau et al. (1995) used various methods, such as Rb–Sr and Sm–Nd whole-rock (carbonatite and fenites) isochron, and U–Pb mineral geochronology to obtain dates, which ranged from 900–950 Ma (Rb–Sr and K–Ar) to 1200–1400 Ma (Sm–Nd and U–Pb). They (Gruau et al. 1995) interpreted the 1200–1400 Ma dates as the age of magmatic emplacement and the 900–950 Ma age as a high-temperature metamorphic event that reset the Rb–Sr and

K–Ar systematics. On the basis of Pb isotope ratios for whole-rock carbonatites, Schleicher et al. (1997) obtained much older secondary isochron ages of 1585±50 Ma and 22 Ga for the ankeritic and dolomitic carbonatites, respectively. Interestingly, the samples from Newania are characterized by extremely high Pb isotope ratios ($^{206}Pb/^{204}Pb$ range from 60 to >500), which are much higher than those for other igneous rocks and carbonatites. These new geochronological data put into question the 959 Ma age from Deans and Powell (1968), and suggest that the Newania carbonatite complex may be older than previously recognized.

The Newania carbonatite is unique amongst Indian carbonatites because of its highly magnesian composition (some samples contain up to 19 wt% MgO; Viladkar and Wimmenauer 1986). Experimental studies investigating the nature of small degree partial melts associated with metasomatized mantle peridotite at pressures of 21 to 30 kbar and temperatures of 930° to 1080°C show that dolomitic (~14 wt % MgO) carbonatite magma may coexist with a mantle peridotite assemblage (e.g. Sweeney 1994; Harmer and Gittins 1998; Lee and Wyllie 1998; Wallace and Green 1988). Phlogopite–carbonate-bearing peridotite will produce more magnesian melt compositions with increasing pressure, which may be attributed to a change in carbonate mineralogy from dolomite to magnesite at about 32 kb (Brey et al. 1983; Olafsson and Eggler 1983). While most global carbonatite occurrences are predominantly Ca-rich and Mg-poor (average MgO content of 1.80 wt%; Woolley and Kempe 1989), other complexes such as Sarfartoq (Greenland), and Sevathur, Tamil Nadu (India) do consist predominantly of dolomitic carbonate (MgO contents > 14 wt%). These occurrences, in addition to the Newania carbonatites, may also be regarded as candidates for direct, partial melts from the mantle. Another noteworthy feature of the Newania carbonatite complex is the presence of graphite as part of the carbonatite mineral assemblage. The co-existence of reduced carbon with gaseous CO_2 and carbonate minerals such as dolomite and magnesite in peridotite mantle is controlled by fO_2 and PT-conditions.

We report here the results of mineralogical study of Newania dolomitic carbonatites (rauhaugites) and data obtained from mineral geothermometers, combined with oxygen and fluorine fugacity determinations. We discuss the mineralogical features and source characteristics of the dolomitic carbonatites and emphasize the co-existence of graphite and mantle carbonates (magnesite, dolomite). Additionally we describe the evolution of fO_2 and HF through the crystallization history of the Newania dolomitic carbonatites.

Geological setting

Dolomitic carbonatite (rauhaugite) is the main type of carbonatite at Newania, and it forms an oblong-shaped exposure that appears to have been emplaced as multiple intrusions (Fig. 1). The main outcrop strikes WNW with an average dip of 40°SSW. Emplacement of carbonatite has not caused any structural disturbance of the surrounding rocks, and thus appears to have occupied a zone of structural weakness within the Precambrian gneiss. The rauhaugite is marked by the presence of abundant, distorted bands and lenses of apatite varying in thickness from a few centimeters to >12 cm. Banding is accentuated by the presence of amphibole, phlogopite and fenitized basement gneiss. The dolomitic carbonatite is intruded by numerous veins of ankeritic carbonatite, and the process has been accompanied by metasomatic replaced of the dolomitic carbonatite along the intrusive contact. The replacement zones contain amphibole and phlogopite, which have been subsequently converted to chlorite, showing that the ankeritic carbonatite melt was H_2O-bearing. A few dykes of ankeritic carbonatite also occur in the fenite zone and extend into the main carbonatite body. A third generation of thinner carbonatite (ankerite + siderite) dykes seems to have intruded much later and are characterized by a sharp contact with the host fenite and a dark brown to almost black colour.

The fenite zone extends for about 100 m beyond the carbonatite and granite-gneiss contact, wherein amphibole-rich areas have developed. About 20 m away from the contact, the fenite becomes more leucocratic and further away eventually grades into pure potassic fenite.

Petrography

The Newania dolomitic carbonatites are fine- to medium-grained, massive and banded rocks containing crystals and grains of amphibole and apatite. In the fine-grained types the groundmass consists of dolomite grains, 2–5 mm in size, with phlogopite, Fe-magnesite and columbite as minor minerals. Monazite, ilmenite, aegerine, pyrrhotine, molybdenite, zircon, bismite, carbocernaite, pyrochlore, baryte and rutile are accessory minerals. Amphibole and phlogopite form thin bands and amphibole contains rare relics of early pyroxene. Pyrochlore is dark brown to almost opaque and occurs as tiny, rounded grains, or lumps of grains frequently associated with phlogopite-rich bands. Rare grains of zircon and Nb-silicate are also observed in these bands. Magnesite forms rare, rounded to euhedral or subhedral grains (Fig. 2a, b), 0.5–1.5 mm in size, in the dolomite matrix and was replaced by siderite along cracks, cleavage cracks and around the rim of grains. Siderite is associated with secondary iron oxide (limonitic oxide), pyrite, and Ba and Sr sulphates. Apatite coexists with phlogopite, amphibole and columbite (Fig. 2c) and occurs as single grains as well as in bands and lenses, with solid inclusions of columbite and graphite. Monazite is

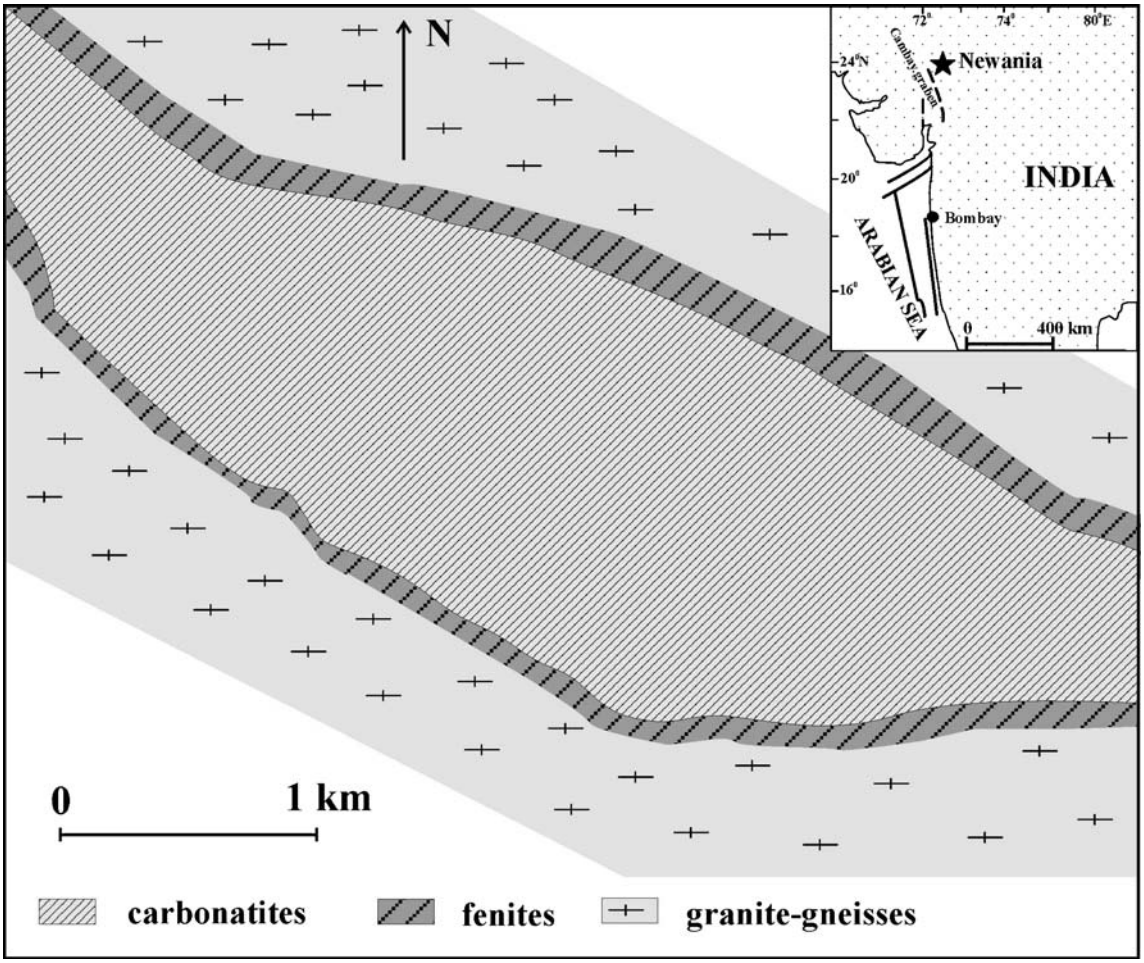

Fig. 1 Simplified geological map of the Newania carbonatite based on Viladkar (1998)

often secondary and forms a thin shell around apatite grains (Fig. 2d). Graphite forms flakes disseminated throughout the carbonatite and also occurs as solid inclusions in apatite, amphibole, magnetite and columbite, and sometimes as a thin shell around magnetite grains (Fig. 3). Magnetite occurs as well developed crystals and rounded or anhedral grains, 2–3 mm in size, that contain irregular and poikilitic inclusions of dolomite and apatite (Fig. 2e, f). Magnetite grains usually contain external composite ilmenite with trellis lamellae along {111} planes (Fig. 2g, h). Ilmenite also occurs as fine grains within the dolomite matrix. Most of the magnetite grains are oxidized, with the formation of hematite suggesting that oxidation occurred at low pressure and below 600°C (Haggerty 1991a).

Analytical methods

Minerals were analyzed using electron probe micro-analysis (a MAR-3 WDS microprobe with an accelerating voltage of 20 kV, beam current of 40 nA, beam size of 3–4 μm and a 20 s counting time) and a LEO-1430 scanning electron microscope with an IncaEnergy-300 energy-dispersive system (SEM-EDS) operated at 20 kV and 0.5 nA. Analyses were carried out at the Geological Institute SB RAS.

Microprobe data for phlogopite were recalculated on the basis of 12 oxygens. Fe^{3+} and Fe^{2+} in minerals were estimated according to Brod et al. (2001). All cations for amphibole were recalculated to 23 oxygen; Fe^{3+} and Fe^{2+} in the mineral was recalculated according to the method described by Robinson et al. (1982).

Mineral compositions

Dolomite

The dominant mineral composition is ferroan dolomite (Fig. 4, Table 1) with 5.47–12.61 wt. % FeO, 0.4–1.1 wt. %

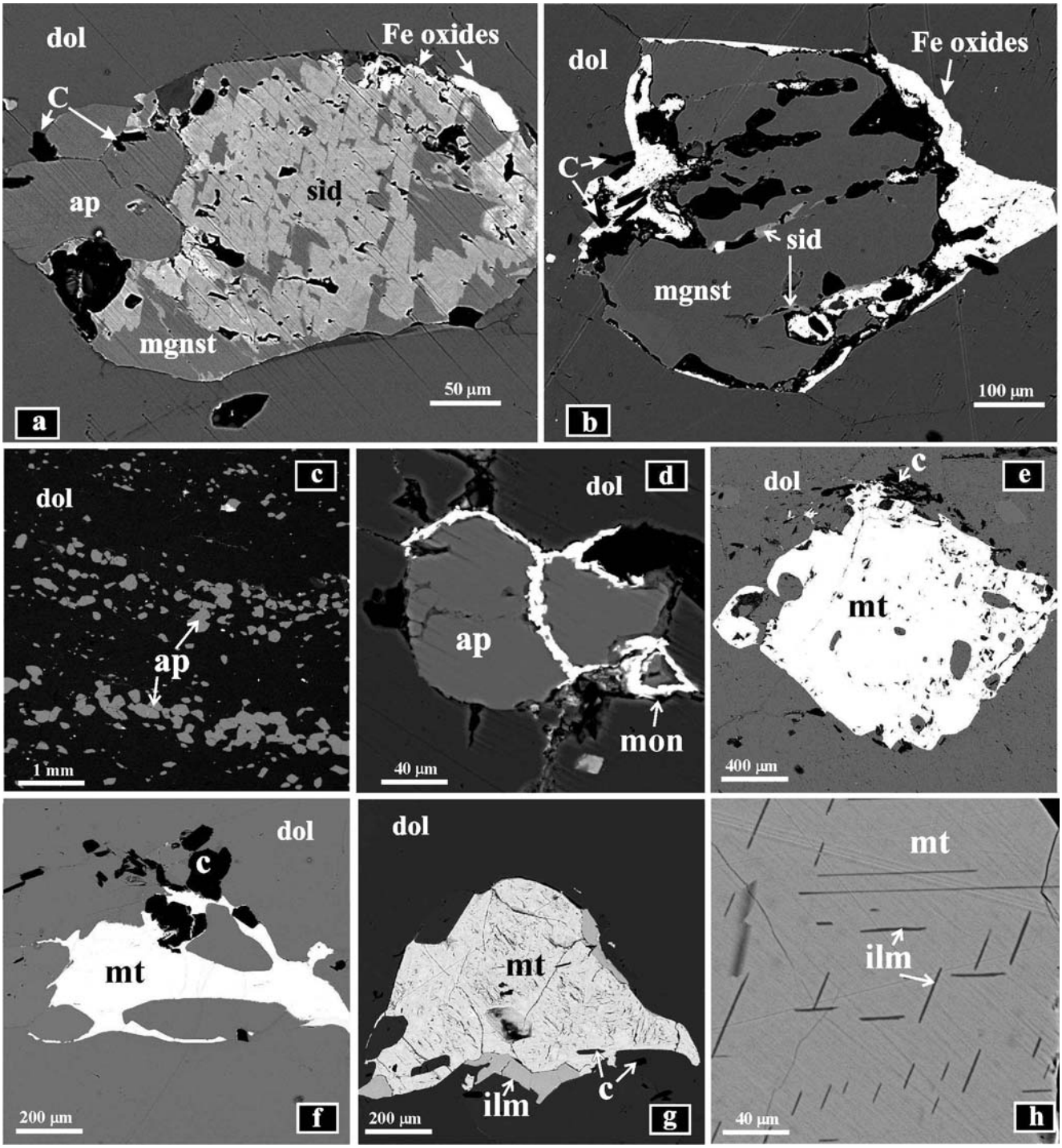

Fig. 2 Mode of occurrence of magnesite (mgnst), apatite (ap) and magnetite (mt) in carbonatites from Newania (BSE images). **a**, **b** replacement of magnesite (mgnst) by siderite (sid) with formation of Fe oxides; **c** apatite (ap) bands in dolomite (dol) matrix; **d** thin shell of monazite (mon) around apatite grains; **e, f** crystals and anhedral grains of magnetite; **g** external composite ilmenite (ilm) in magnetite; **h** lamellae of ilmenite in magnetite, *dol* dolomite, **c** graphite

MnO and 0.73–1.37 wt. % SrO. The mineral composition is similar to dolomite from Sarfartoq (Secher and Larsen 1980), Pogranichnoe and Veseloe (Doroshkevich et al. 2007a, b), which are mantle-like dolomite carbonatites.

Magnesite–siderite

Selected analyses of magnesite and siderite are presented in Table 1 and the results plotted in terms of $CaCO_3$-$MgCO_3$-

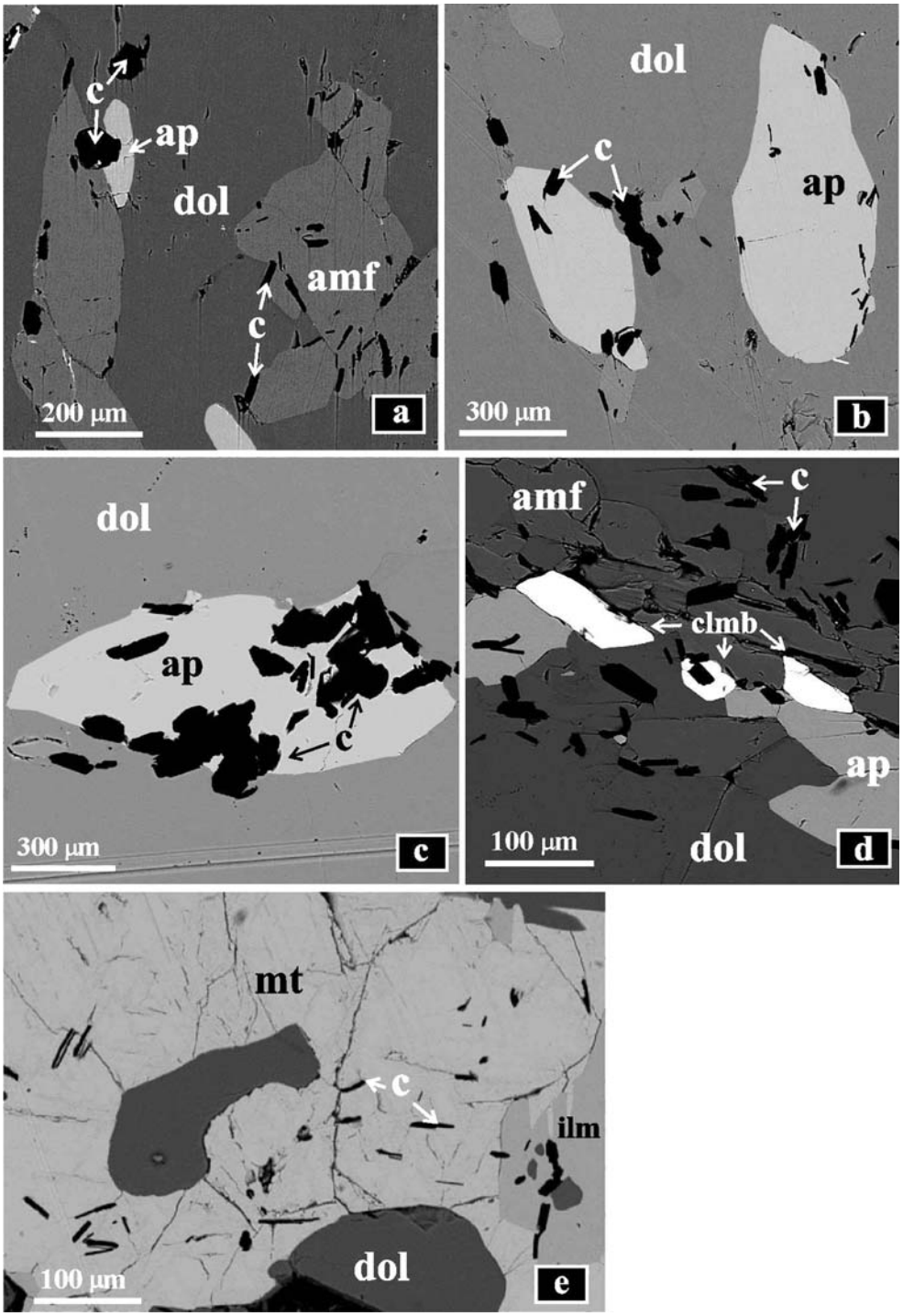

Fig. 3 Distribution of graphite (**c**) in Newania carbonatites (BSE images). *ap* apatite, *dol* dolomite, *amf* amphibole, *clmb* columbite, *mt* magnetite, *ilm* ilmenite

$FeCO_3$ on Fig. 5. Magnesite is ferroan magnesite and siderite is magnesium siderite. Both magnesite and siderite contain a small amount of MnO and CaO. CaO/(CaO+MgO) varies from 0.01 to 0.04. There is a narrow range of Fe:Mg ratios in magnesite, as previously obtained by Buckley and Woolley (1990). Fe: Mg ratios in the mineral vary from 1.1 to 1.6. However, Fe: Mg ratios varied from 2.7 to 9.0 in magnesium siderite. Comparison of magnesite with Lueshe and Kangankunde hydrothermal magnesite–siderite carbonates (Buckley and Woolley 1990) shows higher amounts of Ca and Sr for the latter.

Apatite

Apatite is fluorapatite with F content up to 4.93 wt. %, typical for carbonatites, It is strontium-rich (SrO is up to

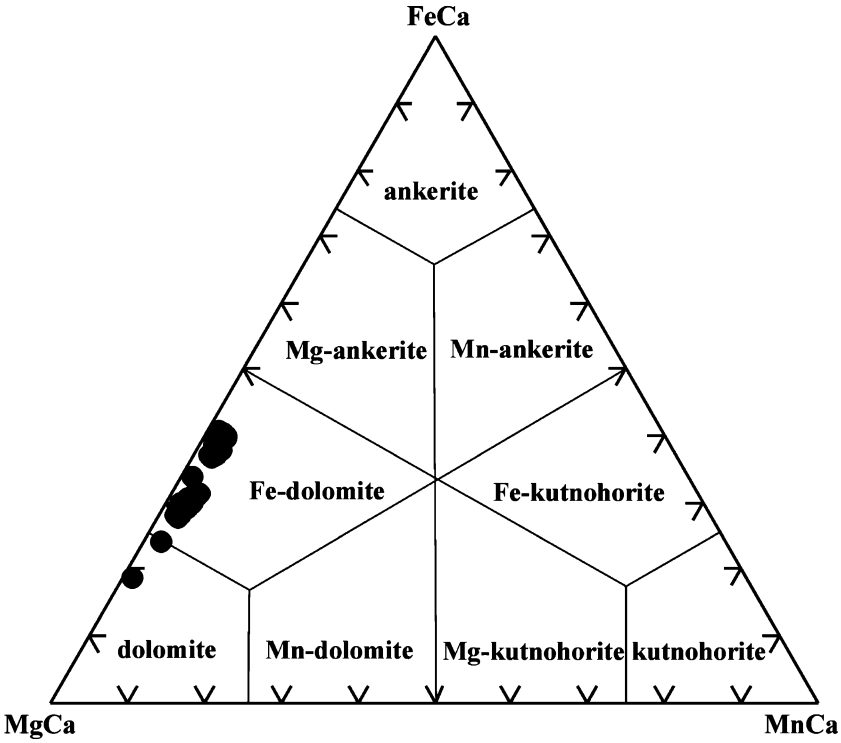

Fig. 4 The triangular classification diagram of Trdlicka-Hoffman (1976) showing the composition (mol. %) of carbonates of the dolomite–ankerite series from the Newania carbonatites

2.9 wt. %) and is slightly enriched in Na_2O, FeO and MgO (Table 2). REE concentrations are low, and below EPMA detection limits. Cl does not exceed 0.11 wt. %. Main and trace element data on the Newania apatites are largely in accordance with the data for Sarfartoq, Pogranichnoe and Veseloe apatites although the Pogranichnoe and Veseloe apatites have higher concentrations of REE than those analyzed for Newania.

Phlogopite

Mica composition (Table 3) is characterized by higher Fe/Fe+Mg (2.7–3) and TiO_2 (up to 1.1 wt. %). Fe^{3+}/Fe^{2+} ratios vary from 1.5 to 2.9. The F content ranges from 2.6 to 2.9 wt. %. Some mica has K_2O contents as low as 6.6 wt. %, suggesting an incipient chloritisation, which is in accordance with petrographic and electron microscope observations. The

Table 1 Representative analyses of carbonate minerals, Newania carbonatites

Mineral	Dolomite			Av (79)	Magnesite			Av (13)	Siderite			Av (19)
Weight percent oxides												
CaO	26.60	27.54	26.54	27.02	1.04	1.16	0.35	0.84	b.d.	b.d.	0.52	0.41
MgO	14.42	16.62	13.27	14.22	21.35	23.65	25.33	22.72	5.64	16.21	12.44	11.06
MnO	0.67	0.75	0.75	0.79	1.34	1.42	1.04	1.44	1.31	1.48	1.89	1.57
FeO	11.5	7.05	12.61	11.11	31.22	32.57	26.77	31.34	50.66	40.49	45.06	45.41
SrO	1.47	0.90	1.07	1.06	b.d.	b.d.	b.d.	–	b.d.	b.d.	b.d.	–
Total	54.66	52.86	54.69		54.95	58.8	53.49		57.61	58.18	59.91	
Molar %												
$CaCO_3$	47.7	50.2	47.7	48.8	1.9	1.9	0.6	1.5	–	–	0.9	0.7
$MgCO_3$	30.4	35.6	28.9	30.2	45.1	46.5	53.8	48.4	12.3	33.4	25.4	23.5
$MnCO_3$	1.0	1.2	1.2	1.3	2.2	2.2	1.7	2.4	2.2	2.4	3.0	2.6
$FeCO_3$	18.7	11.6	20.5	18.2	50.8	49.3	43.8	51.4	85.4	64.2	70.7	74.5
$SrCO_3$	2.1	1.3	1.5	1.5	–	–	–	–	–	–	–	–
Ca/(Ca+Mg)	0.61	0.58	0.62	0.62	0.05	0.05	0.01	0.04	–	–	0.04	0.04

b.d. below detection limit; *av* average composition; in brackets- amount of analyses

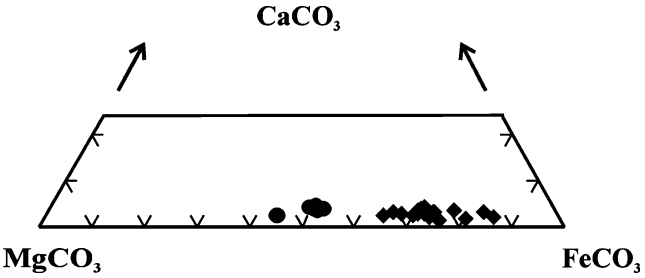

Fig. 5 Composition (mol. %) of carbonates of magnesite–siderite series in the system $CaCO_3$-$MgCO_3$-$FeCO_3$. *Circles*—magnesite, *diamonds*—siderite

average proportions of the phlogopite, annite and siderophillite end-member components in the mica are 54, 33 and 13% respectively.

Magnetite and hematite

Representative compositions of magnetite and hematite are given in Table 4. The bulk of magnetite is dominated by the magnetite end-member composition with minor proportions of the ulvospinel (up to 5.65 wt. % of TiO_2) and magnesioferrite (up to 0.32 wt. % of MgO) series. Magnetite is enriched in chromium (from 0.39 to 1.38 wt. %) and V_2O_3 (0.09–0.28 wt. %) but nickel and cobalt are below detection limits. Hematite that formed by oxidation of magnetite at the postmagmatic stage has similar Ti, Cr, Mg and V contents to the magnetite (Table 4). While magnetite from carbonatites is usually relatively depleted in trace elements such as Ni, Cr and V (Reguir et al. 2008), a similar range of V and Cr values was determined for mantle-derived xenocrysts of magnetite from Veseloe dolomite carbonatites (Doroshkevich et al. 2007b).

Ilmenite

The ilmenite is characteristically depleted in chromium (0.08–0.16 wt. %) and enriched in vanadium (0.29–0.83 wt. %) relative to magnetite (Table 4) and it is characterized by elevated Nb_2O_5 (0.16–1.88 wt. %) and MnO (0.70–1.23 wt. %). Ilmenite has low (up to 2) mole % geikielite.

Pyroxene

Pyroxene occurs as rare isolated grains that is, in places, replaced by amphibole. Compositionally, it is aegirine with minor amounts of Al_2O_3 and CaO (Table 5). Fe^{3+} is predominant in FeO_{total}. The composition of aegirine is similar to that in Pogranichnoe dolomite carbonatites (Doroshkevich et al. 2007a). In addition, early pyroxene is also replaced by amphibole at Pogranichnoe.

Amphibole

The composition of amphibole varies from magnesio-arfvedsonite to magnesioriebeckite. It is TiO_2 and Al_2O_3 poor (Table 5), but enriched in F (1.34–2.07 wt. %). Fe^{3+}/Fe^{2+} ratios vary from 0.5 to 1.0. Its composition is similar to that in mantle-like dolomite carbonatites: Amphibole from Veseloe carbonatites is magnesioriebeckite; amphibole from Pogranichnoe and Sarfartoq carbonatites is magnesio-arfvedsonite.

Temperature and oxygen–hydrogen fluoride fugacity estimates for Newaina carbonatites

Estimates of crystallization temperature were obtained from coexisting apatite–phlogopite and ilmenite–magnetite pairs, using the apatite–biotite thermometer of Ludington (1978) and the Fe–Ti oxide geothermometers of Powell and Powell (1977), Spencer and Lindsley (1981), Andersen and Lindsley (1985) and Ghiorso and Sack (1991).

The apatite–biotite geothermometer yielded temperature estimates in the range 693–978°C. Estimates of the relative HF fugacity, log (fHF/$f$$H_2O$), were calculated using the method of Andersen and Austrheim (1991) and, using the apatite–phlogopite equilibrium temperature, yielded values between (−3.6) and (−4.9). The negative correlation between log (fHF/$f$$H_2O$) and temperature that accompanies the relatively sharp cooling trend illustrated in Fig. 6 reflects buffering of the hydrogen fluoride fugacity by apatite during the evolution of magma. The estimated relative HF fugacity of the Fen carbonatites (Andersen and Austrheim 1991) and the carbonate-rich lamprophyres of

Table 2 Representative analyses of apatite, Newania carbonatites

CaO	Na_2O	MgO	FeO	SrO	Ce_2O_3	La_2O_3	Pr_2O_3	Nd_2O_3	P_2O_5	F	Cl	Total	F=−O_2
Weight percent oxides													
54.33	0.25	b.d.	0.63	1.18	0.58	0.20	b.d.	b.d.	41.99	2.83	b.d.	101.99	1.21
54.16	0.23	b.d.	b.d.	1.21	0.51	0.19	b.d.	0.29	41.29	3.94	b.d.	101.82	1.65
53.96	0.25	b.d.	b.d.	0.58	0.62	0.19	b.d.	0.29	41.42	3.95	b.d.	101.36	1.66
54.08	0.31	0.25	0.32	2.09	0.20	b.d.	b.d.	b.d.	42.04	2.93	0.06	102.32	1.23
53.23	0.30	0.23	0.11	2.19	0.23	b.d.	b.d.	b.d.	41.88	2.50	0.11	100.83	1.05

Table 3 Representative analyses of mica, Newania carbonatites

Weight percent oxides									
SiO_2	38.33	40.71	40.30	42.24	40.46	40.69	39.55	40.59	41.31
TiO_2	0.90	0.54	0.63	0.34	0.42	0.64	0.65	068	1.10
Al_2O_3	13.18	12.45	12.02	13.20	13.80	11.98	12.96	12.83	13.01
FeO	13.24	14.90	15.00	13.61	13.10	14.98	14.26	14.10	13.06
MgO	17.90	16.62	16.03	16.79	16.85	16.53	14.97	17.84	18.01
CaO	b.d.	b.d.	0.57	0.43	0.42	b.d.	0.38	b.d.	b.d.
Na_2O	0.69	0.62	0.99	0.70	0.98	b.d.	b.d.	b.d.	b.d.
K_2O	7.94	9.62	7.70	7.12	6.55	9.40	10.08	10.69	10.88
F	2.71	2.55	2.68	2.49	2.79	2.83	2.90	2.84	2.62
$F=-O_2$	1.14	1.07	1.13	1.05	1.17	1.19	1.22	1.19	1.10
Total	94.98	98.01	95.92	96.92	95.37	97.05	95.75	99.75	99.99
Structural formulae based on 12 oxygen									
Si	2.91	3.05	3.06	3.09	3.01	3.05	3.02	2.97	2.99
^{IV}Al	1.09	0.95	0.94	0.91	0.99	0.95	0.98	1.03	1.01
T site total	4.0	4.0	4.0	4.0	4.0	4.0	4.0	4.0	4.0
^{VI}Al	0.09	0.12	0.13	0.23	0.22	0.11	0.18	0.08	0.10
Fe^{2+}	0.23	0.31	0.37	0.33	0.31	0.34	0.38	0.23	0.20
Fe^{3+}	0.61	0.60	0.58	0.50	0.51	0.60	0.53	0.63	0.59
^{VI}Mg	2.03	1.81	1.81	1.83	1.87	1.85	1.70	1.95	1.94
Ti	0.05	0.03	0.04	0.02	0.02	0.04	0.04	0.04	0.06
O site total	3.01	2.87	2.93	2.91	2.93	2.94	2.83	2.93	2.89
Ca	–	–	0.05	0.03	0.03	–	0.03	–	–
Na	0.10	0.09	0.10	0.10	0.14	–	–	–	–
K	0.77	0.93	0.76	0.68	0.64	0.92	0.98	0.99	1.03
A site total	0.87	1.01	0.96	0.81	0.82	0.92	0.98	0.99	1.03
Total cations	7.88	7.89	7.77	7.72	7.75	7.85	7.84	7.92	7.92
F	0.67	0.64	0.67	0.62	0.70	0.71	0.73	0.71	0.66
OH	1.33	1.36	1.33	1.38	1.30	1.29	1.28	1.29	1.35

n.a. not analyzed; total without theoretical H_2O (4.5 wt. %)

the Torngat and Ailik Bay (Tappe et al. 2006) is lower than that for Newania carbonatites. Nevertheless, at higher relative HF fugacity conditions Newania apatites crystallized over a narrow temperature interval and, at lower relative HF fugacity conditions, there is partial overlap with Fen carbonatite near "solidus" crystallization field (~700–600°C) determined by Wyllie (1966).

Temperature and oxygen fugacity were calculated for ilmenite–magnetite pairs using the ILMAT-1.20 (Powell and Powell 1977; Spencer and Lindsley 1981; Andersen

Table 4 Representative analyses of oxide minerals, Newania carbonatites

Mineral	magnetite	Av (23)	hematite	ilmenite	Av (18)							
Weight percent oxides												
TiO_2	0.13	0.49	0.27	5.65	2.51	0.13	0.41	50.20	50.71	50.82	49.04	50.13
Cr_2O_3	1.29	0.60	0.99	0.36	0.71	0.43	0.48	0.15	0.08	0.16	0.05	0.09
FeO	91.91	92.56	90.83	85.29	91.50	88.12	88.83	46.82	46.05	46.94	46.77	46.62
MnO	b.d.	b.d.	b.d.	b.d.	–	b.d.	b.d.	1.14	1.12	1.11	0.88	1.01
MgO	0.27	0.26	0.29	0.29	0.28	0.26	0.28	0.56	0.49	0.50	0.40	0.42
V_2O_3	0.14	0.09	0.14	0.14	0.15	0.14	0.12	b.d.	b.d.	b.d.	0.82	0.38
Nb_2O_5	b.d.	b.d.	b.d.	b.d.	–	b.d.	b.d.	0.65	0.55	0.16	1.88	0.87
Total	93.74	93.99	92.67	92.05		89.07	90.13	99.52	99.00	99.69	99.79	

Table 5 Representative analyses of amphibole and pyroxene, Newania carbonatites

Mineral	Magnesio-arfvedsonite/magnesio-riebeckite								Aegerine	
Weight percent oxides										
SiO_2	56.48	55.22	56.86	56.62	56.85	54.50	54.41		54.22	53.94
TiO_2	0.09	0.07	0.10	0.11	0.09	0.08	0.09		b.d.	b.d.
Al_2O_3	0.23	0.21	0.24	0.24	0.22	0.95	1.03		1.09	1.08
FeO	12.01	13.16	14.27	11.88	11.97	24.05	22.57		29.04	30.12
MnO	0.12	0.11	0.07	0.11	0.09	0.09	0.08		b.d.	b.d.
MgO	16.37	15.67	14.66	16.42	16.06	8.91	10.07		0.98	b.d.
CaO	3.91	2.22	2.30	3.79	3.26	0.52	0.38		0.68	0.69
Na_2O	6.16	7.50	6.81	6.16	6.55	7.14	7.75		13.82	14.13
K_2O	2.45	2.65	2.90	2.53	2.66	0.20	0.26		b.d.	b.d.
F	1.63	1.34	1.09	2.07	1.55	1.20	1.30		–	–
Total	99.45	98.15	99.30	99.93	99.25	97.64	97.94		99.83	99.96
$F=-O_2$	0.68	0.56	0.46	0.87	0.65	0.50	0.55		–	–
Structural formulae based on 23 oxygen for amphibole and 6 oxygen for pyroxene										
Si	8.04	7.98	8.12	8.12	8.10	7.95	7.89	Si	1.99	1.99
Al	–	0.02	–	–	–	0.05	0.11	Al	0.006	0.01
T site total	8.04	8.0	8.12	8.12	8.10	8.0	8.0	T site total	2.0	2.0
Al	0.04	0.01	0.04	0.04	0.04	0.11	0.07	Al	0.04	0.04
Fe^{3+}	0.53	0.71	0.59	0.73	0.45	1.70	1.68	Fe^{3+}	0.89	0.93
Ti	0.01	0.01	0.01	0.01	0.01	0.01	0.01	Mg	0.05	–
Mg	3.47	3.38	3.12	3.42	3.41	1.94	2.18	M1 site total	0.98	0.97
Fe^{2+}	0.89	0.88	1.12	0.70	0.98	1.23	1.06	Ca	0.03	0.03
Mn	0.02	0.01	0.01	0.01	0.01	0.01	0.01	Na	0.98	1.01
C site total	4.96	5.0	4.89	4.95	4.9	5.0	5.0	M2 site total	1.01	1.04
Na	1.44	1.66	0.24	1.66	0.39	1.92	1.94	Total cations	3.99	4.01
Ca	0.56	0.34	1.76	0.34	1.61	0.08	0.06			
B site total	2.0	2.0	2.0	2.0	2.0	2.0	2.0			
Ca	0.04	–	0.12	0.12	0.10	–	–			
Na	0.26	0.45	0.12	0.06	0.21	0.10	0.24			
K	0.44	0.49	0.53	0.37	0.48	0.04	0.05			
A site total	0.74	0.94	0.77	0.55	0.79	0.14	0.29			
Total cations	15.74	15.94	15.78	15.62	15.79	15.14	15.29			
F	0.73	0.61	0.49	0.91	0.70	0.55	0.60			
OH	1.27	1.39	1.51	1.09	1.30	1.45	1.40			

Total for amphibole is without theoretical H_2O (2.0 wt. %)

and Lindsley 1985) and MELTS (Ghiorso and Sack 1991) programs. ILMAT-1.20 gave temperature estimates for ilmenite–magnetite pairs from 463°C to 669°C. However, the MELTS program gave lower estimates for temperature. For example, for magnetite with 2.51 and 5.65 wt. % TiO_2, the ILMAT-1.20 model gives 582°C and 669°C, compared with 353°C and 426°C respectively for the MELTS model. At 5.65 wt. % of TiO_2 ILMAT produces $\log_{10}fO_2$ of (−17.35), whereas MELTS yields $\Delta\log fO_2$ of NNO (−2.68). Probably, the thermometry is uncertain due to the acute intersection angle of the thermoisopleths and the effect of errors in the models. The fO_2 calculations are more accurate and results vary from FMQ −1.5 to FMQ +3.5 (log-bar unit deviation from FMQ buffer) (Fig. 7). The results indicate that the Newania source mantle existed under fairly oxidized conditions. The oxidation state is embodied in the presence of Fe-columbite, and composition of phlogopite, amphibole and pyroxene that have higher Fe^{3+} content. In addition, the range of fO_2 values corresponds to elemental carbon stability in the system. It indicates that the Newania source could be in equilibrium with free carbon. This conclusion is confirmed by the presence of fine-grained graphite crystals in minerals. Furthermore, carbonate (magnesite) and reduced carbon (graphite) were

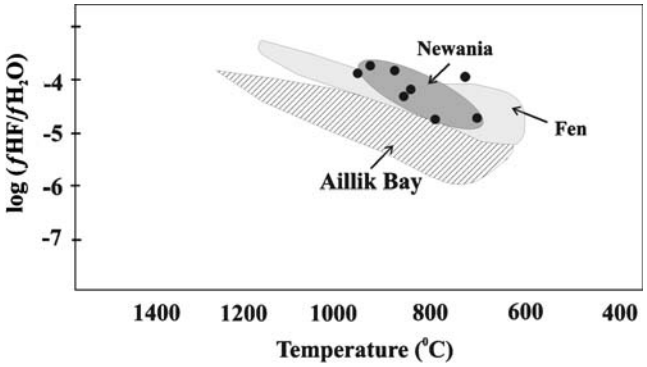

Fig. 6 Relative HF fugacity log (fHF/fH_2O) vs equilibration temperature (°C) calculated for apatite–phlogopite pairs from Newania. Field for Fen is from Andersen and Austrheim (1991); field for Aillik Bay is from Tappe et al. (2006)

co-existing early magmatic phases at Newania. Both the oxidized and reduced forms of carbon can be stable in the mantle depending on oxygen fugacity as well as pressure, temperature and fluid composition. The oxygen fugacity values for magnesite–graphite assemblages in the Newania based on our temperature calculations (~800°C–900°C) lie approximately on the CCO buffer of Frost (1991) and have negative deviation from FMQ (FMQ −0.5 to −1) (Fig. 7). The occurrence of post-magmatic hematite (that formed by oxidation of magnetite) indicates that oxygen fugacity increased up to the HM buffer during a later (postmagmatic) stage of Newania carbonatite evolution (Fig. 7).

Discussion

Mantle source characteristics

The features of Newania carbonatites as primary mantle-derived melt such as high Mg#s of carbonatites (up to 19 wt. % of MgO), low initial Sr^{87}/Sr^{86} ratios (0.7021),

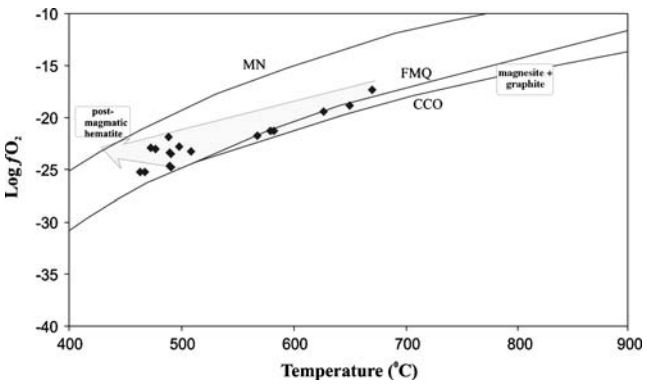

Fig. 7 Log *fO2*–T diagram showing the Newania trend relative to the common petrologic buffers. Hematite and magnesite–graphite fields indicate approximate conditions

mantle-like C and O isotope ratios (−5.1 and 8.1), have been described by Viladkar (1998). Nd isotope studies (Gruau et al. 1995) and analyses of noble gases and N (Basu and Murty 2006) in Newania carbonatites also indicate a mantle source.

It is well known that a dolomite carbonatite would be the most likely candidate for a primary magma composition derived from carbonated mantle peridotite (e.g. Sweeney 1994; Harmer and Gittins 1998; Lee and Wyllie 1998). Newania carbonatite certainly fulfills most of the criteria for a directly-derived primary carbonatite magma as the dolomite composition is consistent with that of experimentally produced carbonatitic melts in equilibrium with mantle minerals. According to experimental results (e.g. Sweeney 1994), silica should be relatively high, 1.5–12.7 wt. %, in directly-derived melts and, although the Newania silica contents are 1.00 wt. %, the Newania carbonatites do always contain igneous silicate minerals such as amphibole, pyroxene and phlogopite. CaO/(CaO+MgO) in Newania carbonatites varies from 0.6 to 0.76 and exhibits greatest similarity with experimental carbonatite melt in equilibrium with a spinel harzburgite (Dalton and Wood 1993).

Constraints on the mineralogy

The key features of the Newania carbonatites are the presence of magnesite, graphite and Cr-magnetite.

Magnetite in carbonatites is usually relatively poor in chromium with the maximum Cr content (0.65 wt. %) in magnetite detected in silicocarbonatite from Kontozero, Russia (Reguir et al. 2008). Significantly higher Cr content has been reported in mantle-derived xenocrysts of magnetite from carbonatites (e.g., Woolley et al. 1991; Doroshkevich et al. 2007b) and kimberlites (e.g. Haggerty 1991b). Often reaction of these xenocrysts with carbonatite magma can produce a rim of magnetite enriched in Cr (e.g. Doroshkevich et al. 2007b). Newania magnetite shows higher Cr content (0.39–1.38 wt % Cr_2O_3) than that normally observed in carbonatites (Reguir et al. 2008) but it is not xenocrystic. Petrographic evidence clearly points to co-existence of magnetite with the carbonate minerals and there is no evidence of contamination. Newania magnetite composition can therefore be interpreted unequivocally as Cr-enrichment of primary carbonatite melt that was directly derived from carbonated mantle peridotite.

Newania magnesite composition is in agreement with that of Buckley and Woolley (1990) and it is interpreted as the earliest crystallizing primary mineral. Experiments have shown that magnesite is a stable carbonate phase in the mantle, for example, at pressure from 3 to 7 GPa, (Dalton and Presnall 1998). Furthermore, carbonate melt that is in equilibrium with lherzolite in the magnesite stability field has a dolomitic composition (Dalton and

Presnall 1998). Support for this experimental data is provided by the presence of magnesite inclusions in natural diamond from the Finsch kimberlite (South Africa) (Wang et al. 1996) and from the Mir kimberlite (Russia) (Bulanova and Pavlova 1987). Clearly, the carbonate chemistry is dependent on the composition of the source as well as the PT conditions. Experiments (Dalton and Presnall 1998) and natural observations (Wang et al. 1996) show that Ca decreases in co-existing magnesite and carbonate melt with increasing pressure; and the Newania magnesites and carbonatite melt have a similar Ca content to those of experiments.

There are several reports of graphite in carbonatite worldwide (e.g. Verwoerd 1967; Worley and Cooper 1995; Doroshkevich et al. 2007a). The possible mechanisms by which graphite occurs in carbonate rocks are incorporation of xenocrysts, precipitation from carbonate melt, breakdown of Fe carbonates, and metamorphic reaction. Newania graphite is in textural equilibrium with apatite, columbite, amphibole, and dolomite, and is interpreted to coexist with carbonatite minerals, having precipitated from carbonate magma. The estimated temperatures for apatite crystallization support a high temperature for graphite formation. Although thermal disequilibrium between Fe-carbonate (magnesite, dolomite) and magnetite is theoretically possible, this scenario does not fit with the petrographic evidence as (a) graphite occurs as solid inclusions in all carbonatite minerals, including magnesite; and (b) there does not seem to be break down of magnesite with magnetite formation, but that magnesite has undergone post-magmatic recrystallizion to form siderite plus limonitic oxides. The formation of elemental carbon (graphite and/or diamond) in a carbonate (dolomite or magnesite)-silicate system has been studied in numerous experiments (e.g. Sokol et al. 2001; Pal'yanov et al. 2005), and in the peridotite$_{30}$–dolomite$_{70}$ (wt. %) system at P=7 GPa and T= 1200–1800°C by Bobrov and Litvin (2007). Results of the experiments indicated that dolomite melts in the mantle enriched in H_2O and CO_2 promote the formation of elemental carbon; and the main parameters governing the process of diamond/graphite formation are temperature, pressure and oxygen fugacity. At appropriate conditions, diamond and graphite can crystallize in melt as well as in subsolidus fluids.

Oxidation state of the Newania source

Oxygen fugacity values in the mantle vary within a range of 5–6 log units relative to FMQ (Haggety and Tompkin 1983). For example, peridotite xenoliths exhibit a fO_2 range from −1.5 to +1.5 log units relative to FMQ buffer (Wood et al. 1990). Magmatic rocks of ocean islands are highly oxidized (+2 to +3 log units relative to FMQ) (Ballhaus 1993; Kogarko and Ryabchikov 1991). High oxygen fugacities were estimated for carbonatite complexes from Maimecha-Kotuy, Russia (Ryabchikov et al. 2002), Gronnedal-Ika, Greenland (Halama et al. 2005) and Aillik Bay, Labrador (Tappe et al. 2006). The presence of fine-grained graphite crystals in carbonatite minerals shows that the parental source for Newania carbonatites was fairly oxidized but corresponds to elemental carbon stability in the C-O-H system. Oxygen fugacity increased during the crystallization history of Newania relative to the FMQ buffer curve towards values above the HM buffer. However, H_2O and CO_2 would be the dominant volatiles for Newania carbonatites according to the observed evolution of fO_2 values. The species in the fluid will change from predominantly CO_2+H_2O at relatively high oxygen fugacities to CH_4-rich under reducing conditions (Kadik 1997).

Conclusions

1) Newania dolomite carbonatites have features of melts that are directly derived from carbonated mantle peridotite.
2) Magnesite is the earliest crystallizing phase in the Newania carbonatites. Magnetite is relatively Cr-rich and crystallized at temperature 463° to 669°C. Apatite crystallized at higher temperature 700–950°C. Graphite precipitated from carbonate magma at temperatures of at least 700°C.
3) Newania carbonatites are characterized by a relatively high log (fHF/$f$$H_2O$) level.
4) Because a parental magma has the potential to preserve the redox state of its source, it can be inferred that the Newania carbonatites were derived from a fairly oxidized mantle region and that there was increasing oxygen fugacity during magmatic evolution.

Acknowledgment The studies have been carried out with the support of the Integral project of RAS (ONZ 10.3), RFFR (grant 08-05-98028) and INTAS grant 05-1000008-7938. We are grateful to Nikolay Karmanov and Sergey Kanakin for help with electron microprobe analysis at the Geological Institute SB RAS (Russia). The authors much appreciate useful comments and the constructive criticism from Dr. Anatoly Zaitsev. We are indebted to the anonymous referees for reviews. Kathryn Moore is thanked for the correction of the English language.

References

Andersen T, Austrheim H (1991) Temperature-HF fugacity trends during crystallization of calcite carbonatite magma in the Fen complex, Norway. Mineral Mag 55:81–94

Andersen DJ, Lindsley DH (1985) New (and final) models for the Ti-magnetite/ilmenite geothermometer and oxygen barometer. Abstract AGU 1985 Spring Meeting Eos Transactions. Am Geophys Union 66(18):416

Ballhaus C (1993) Redox states of lithospheric and asthenospheric upper mantle. Contrib Mineral Petrol 114:331–348

Basu S, Murty SVS (2006) Noble gases and N in carbonatites from Newania, India: Pristine N in subcontinental lithosphere, *Abstracts of Goldschmidt Conference*, A40

Bobrov AV, Litvin Yu A (2007) Formation of diamond in peridotite–carbonate-carbon melts at 7.0–8.5 GPa: concentration barrier and singenesis of silicate inclusions, Vestnik of Earth department of RAS, 1 (25), http://www.scgis.ru/russian/cp1251/h_dgggms/1-2007/informbul-1_2007/term-10.pdf

Brey G, Brice WR, Ellis DJ, Green DH, Harris KL, Ryabchikov ID (1983) Pyroxene-carbonate reactions in the upper mantle. Earth Planet Sci Lett 62:63–74

Brod JA, Gaspar IC, de Arajo DP, Gibson SA, Thompson RN, Junqueira-Brod TS (2001) Phlogopite and tetra-ferriphlogopite from Brasilian carbonatite complexes: petrogenetic constraints and implications for mineral-chemistry sistematics. J Asian Earth Sci 19:265–296

Buckley HA, Woolley AR (1990) Carbonates of the magnesite–siderite series from four carbonatite complexes. Mineral Mag 54:413–418

Bulanova GP, Pavlova LP (1987) Magnesite form peridotite mineral association in a diamond from the Mir pipe. Dokl Earth Sci 295:176–179

Dalton JA, Presnall DC (1998) The continuum of primary carbonatitic–kimberlitic melt compositions in equilibrium with lherzolite: data from system CaO-MgO-Al2O3-SiO2-CO2 at 6 GPa. J Petrol 39:1953–1964

Dalton JA, Wood BJ (1993) The compositions of primary carbonate melts and their evolution through wallrock reaction in the mantle. Earth Planet Sci Lett 119:511–525

Dar KK (1964) Some geological data on atomic-energy minerals in India. J Geol Soc India 5:112–120

Deans T, Powell JL (1968) Trace elements and strontium isotopes in carbonate, fluorites and limestones from India and Pakistan. Nature 218:750–752

Doroshkevich AG, Wall F, Ripp GS (2007a) Magmatic graphite in dolomite carbonatite at Pogranichnoe, North Transbaikalia, Russia. Contrib Mineral Petrol 153:339–353

Doroshkevich AG, Wall F, Ripp GS (2007b) Calcite-bearing dolomite carbonatite dykes from Veseloe, North Transbaikalia, Russia and possible Cr-rich mantle xenoliths. Mineral Petrol 90:19–49

Frost, D.J. (1991). Introduction to oxygen fugacity and its petrologic importance. In: Lindsley DH (ed) Oxide minerals: petrologic and magnetic significance, Reviews in Mineralogy and Geochemistry, 25, 1–8

Ghiorso MS, Sack RO (1991) Fe-Ti oxide geothermometry: thermodynamic formulation and the estimation of intensive parameters in silicic magmas. Contrib Mineral Petrol 108:485–510

Gruau G, Petibon C, Viladkar S (1995) Extreme isotopic signature in carbonatites from Newania, Rajasthan. Terra Nova 7, Abstract Suppl 1:336

Haggerty SE (1991) Oxide textures—a mini-atlas In: Lindsley DH (ed) Oxide minerals: petrologic and magnetic significance. Rev Mineral Geochem 25:129–137

Haggerty SE (1991b) Oxide mineralogy of the upper mantle. In: Lindsley DH (ed) Oxide minerals: petrologic and magnetic significance. Rev Mineral Geochem 25:355–407

Haggety S, Tompkin S (1983) Redox state of Earth's upper mantle from kimberlitic ilmenites. Nature 303:295–300

Halama R, Vennemann T, Siebel W, Markl G (2005) The Gronnedal-Ika Carbonatite syenite complex, South Greenland: carbonatite formation by liquid immiscibility. J Petrol 46(1):191–217

Harmer RE, Gittins J (1998) The case for primary, mantle-derived carbonatite magma. J Petrol 39:1895–1903

Kadik A (1997) Evolution of Earth's redox state during upwelling of carbon-bearing mantle. Phys Earth Planet In 100:157–166

Kogarko LN, Ryabchikov ID (1991) Redox equilibria in alkaline lavas from Trindade Island, Brazil. Int Geol Rev 36:473–483

Lee W, Wyllie PJ (1998) Petrogenesis of carbonatite magmas from mantle to crust, con-strained by the system CaO-(MgO+FeO*)-(Na_2O+K_2O)-(SiO_2+Al_2O_3+TiO_2)-CO_2. J Petrol 39:495–517

Ludington S (1978) The biotite–apatite geothermometer revisited. Am Mineral 63:551–553

Mishra SP (1982) New genetic model for base metals in the Aravalli Region, India. Symposium on Metallogeny of the Precambrian, I.G.C.P. Project 91, 63-70

Olafsson M, Eggler DH (1983) Phase relations of amphibole, amphibole-carbonate and phlogopite-carbonate peridotite: petrologic constraints on the astenosphere. Earth Planet Sci Lett 64:305–315

Pal'yanov YuN, Sokol AG, Tomilenko AA, Sobolev NV (2005) Conditions of diamond formation through carbonate–silicate interaction. Eur J Mineral 17(2):207–214

Phadke AV, Jhingran AG (1968) On the carbonates at Newania, Udaipur district, Rajasthan. J Geol Soc India 9:165–169

Powell R, Powell M (1977) Geothermometry and oxygen barometry using coexisting iron–titanium oxides. Mineral Mag 41 (318):257–263

Reguir EP, Chakhmouradian AR, Halden NM, Zaitsev AN (2008) Magmatic and reaction trend in magnetite from the Kerimasi carbonatites, Tanzania. *Canadian Mineralogist*

Robinson P, Spear FS, Schumacher JC, Laird J, Klein C, Evans BW, Doolan BL (1982) Phase relations of metamorphic rocks amphiboles: natural occurrences and theory. In: Veblen DR, Ribbe PH (eds) Review in mineralogy, 9B, Amphiboles: Petrology and experimental phase relations. Mineralogical Society of America, Washington, pp 1–267

Ryabchikov ID, Solovova IP, Kogarko LN, Brey GP, Ntaflos Th, Simakin SG (2002) Thermodynamic parameters of generation of meymechites and alkaline picrites in the Maymecha-Kotui Province: evidence from melt inclusions. Geochem Int 40(11):1031–1042

Schleicher H, Todt W, Viladkar SG, Schmidt F (1997) Pb/Pb age determinations on the Newania and Sevathur Carbonatites of India: evidence for multi stage histories. Chem Geol 40:261–273

Secher K, Larsen LM (1980) Geology and mineralogy of the Sarfartoq carbonatite complex, southern West Greenland. Lithos 13:199–212

Sokol AG, Borzdov YuM, Pal'yanov YuN, Khokhryakov AF, Sobolev NV (2001) An experimental demonstration of diamond formation in the dolomite-carbon and dolomite-fluid-carbon systems. Eur J Mineral 13(5):893–900

Spencer KJ, Lindsley DH (1981) A solution model for coexisting iron–titanium oxides. Am Mineral 66(11–12):1189–1201

Sweeney RJ (1994) Carbonatite melt compositions in the Earth's mantle. Earth Planet Sci Lett 128:259–270

Tappe S, Foley SF, Jenner GA, Heaman LM, Kjarsgaard BA, Romer RL, Stracke A, Joyce N, Hoefs J (2006) Genesis of ultramafic lamprophyres and carbonatites at Aillik Bay, Labrador: a consequence of incipient lithospheric thinning beneath the North Atlantic craton. J Petrol 47(7):1261–1315

Trdlicka-Hoffman (1976) Undersuchengen der chemischen Zusammensetzung der gangkarbonate von Kutna Hora (CSSR). Freib Forschung shefte C231:29–81 Freiberg

Verma PK, Greiling RO (1995) Tectonic evolution of the Aravalli Orogen (NW India): An inverted Proterozoic Rift Basin. Geol Rundsch 84:683–686

Verwoerd WJ (1967) The carbonatites of South Africa and South West Africa. Handb GSSA 6:251–252

Viladkar SG (1998) Carbonatite occurrences in Rajasthan, India. Petrology 6(3):272–283

Viladkar SG, Pawaskar PB (1989) Rare earth element abundances in carbonates and fenites of the Newania complex, Rajasthan. Bull Geol Soc Finland 61:113–122

Viladkar SG, Wimmenauer W (1986) Mineralogy and geochemistry of the Newania carbonatite–fenite complex, Rajasthan, India. N Jb Mineral Abh 156:1–21

Viladkar SG, Kienast JR, Fourcade S (1993) Mineralogy of the Newania carbonatite, Rajsthan, India. IAGOD Symposium, Orleans, France, p 55

Wallace ME, Green DH (1988) Experimental determination of primary carbonatite magma composition. Nature 335:343–346

Wang A, Pasteris JD, Meyer HOA, Dele-Duboi ML (1996) Magnesite-bearing inclusion assemblage in natural diamond. Earth Planet Sci Lett 141:293–306

Wood BJ, Bryndzia LT, Johnson KE (1990) Mantle oxidation state and its relationship to tectonic environment and fluid speciation. Science 248:337–345

Woolley AR, Kempe DRC (1989) Carbonatites: nomenclature, average chemical composition, and element distribution. In: Bell K (ed) Carbonatites: genesis and evolution. Unwin Hyman, London, pp 1–14

Woolley AR, Barr MWC, Din VK, Jones GC, Wall F, Williams CT (1991) Extrusive carbonatites from the Uyaynah area, United Arab Emirates. J Petrol 32:1143–1167

Worley BA, Cooper AF (1995) Mineralogy of the Dismal Nepheline Syenite, Southern Victoria Land, Antarctica. Lithos 35:109–128

Wyllie PJ (1966) Experimental studies of carbonatite problems: the origin and differentiation of carbonatite magmas: In: Tuttle OF, Gittins J (eds) Carbonatite. Interscience, New York, pp 311–352